

## *Supplement of:*

# **Sediment transport in Indian rivers high enough to impact satellite gravimetry**

Alexandra Klemme<sup>1</sup>, Thorsten Warneke<sup>1</sup>, Heinrich Bovensmann<sup>1</sup>, Matthias Weigelt<sup>2</sup>, Jürgen Müller<sup>2</sup>, Tim Rixen<sup>3</sup>, Justus Notholt<sup>1</sup>, and Claus Lämmerzahl<sup>4</sup>

<sup>1</sup>Institute of Environmental Physics, University of Bremen, Otto-Hahn-Allee 1, 28359 Bremen, Germany

<sup>2</sup>Institute of Geodesy, Leibniz Universität Hannover, Welfengarten 1, 30167 Hannover, Germany

<sup>3</sup>Leibniz Center for Tropical Marine Research, Fahrenheitstr. 6, 28359 Bremen, Germany

<sup>4</sup>Centre of Applied Space Technology and Microgravity, University of Bremen, Am Fallturm 2, 28359 Bremen, Germany

**Correspondence:** A. Klemme (aklemme@uni-bremen.de)

---

## **Contents**

<b>1</b>	<b>Description of the studied rivers</b>	<b>1</b>
1.1	The Ganges River . . . . .	1
1.2	The Brahmaputra River . . . . .	1
1.3	The Meghna River . . . . .	1
1.4	The Indus River . . . . .	1
<b>2</b>	<b>Challenges in data comparability and necessary assumptions</b>	<b>2</b>
2.1	Scarcity in sediment measurements from the Indian subcontinent . . . . .	2
2.2	Potential impact of GRACE data filtering and leakage . . . . .	3
<b>3</b>	<b>Discussion of data seasonality</b>	<b>4</b>
<b>4</b>	<b>Interpretation of Indus data gap</b>	<b>4</b>
<b>5</b>	<b>Additional figures and tables</b>	<b>6</b>

## **1 Description of the studied rivers**

### **1.1 The Ganges River**

The Ganges River drains a basin of 950,754 km<sup>2</sup> mainly located in India, but also including Nepal as well as parts of China and Bangladesh (Figure 1). The river originates at the Gangotri glacier (7,010 m altitude) in the Uttarakhand Himalaya close to the Tibet-India border (Coleman, 1969; Singh, 1988), descends along the Great and Lesser Himalaya and flows southeast across India. In Bangladesh, it confluences with the Brahmaputra River to form the river Padma, which discharges into the Bay of Bengal (Figure 1). Prior to the 16th century, the majority of water from the Ganges discharged directly into the Bay of Bengal in the western part of the river delta. Over time, the channel migrated northeast to its present position (Coleman, 1969). The total length of the main Ganges River branch from its origin to the sea is about 2,507 km (Akhtar et al., 2009). The river profile shows an initial steep decline along the mountains, followed by about 2,000 km of little slope through the Indo-Gangetic plain (Figure S6). The basin is bounded in the north by the Himalayas and in the south by the Vindhya Range (Singh, 1988).

### **1.2 The Brahmaputra River**

The Brahmaputra River drains a basin of 539,989 km<sup>2</sup> within the countries China, India, Bhutan, and Bangladesh (Figure 1). It originates in Tibet on the north slope of the Himalayas and initially flows eastward to the eastern end of India, where it turns south and then west until it reaches Bangladesh, and confluences with the the Ganges River (Figure 1, Coleman, 1969). The Brahmaputra is a braided river that carries similar amounts of water to the Ganges River but slightly more sediment (Coleman, 1969). Generally flood peaks in the Brahmaputra will occur before the peaks in the Ganges (Coleman, 1969). The total length of the main Brahmaputra river branch is about 3,969 km. In contrast to the Ganges river, its profile shows a slower decline along the mountain branch for about 2,000 km before the steeper decline when leaving the mountain regions and it only flows through floodplain regions for about 1,200 km before discharging into the ocean (Figure S6).

### **1.3 The Meghna River**

The Meghna River is often considered in combination with the Ganges and Brahmaputra rivers. These three rivers confluence in Bangladesh (Figure 1) to form the Ganges-Brahmaputra-Meghna Delta, the Earth's largest and most populous delta system (Paszowski et al., 2021). However, in contrast to the Ganges and Brahmaputra rivers, which are rich in sediment, the Meghna river originates in the Indian Naga Hills at less than 2,000 m elevation and carries comparatively little sediment of  $(6 - 12) \cdot 10^9 \text{ kg yr}^{-1}$  (Rahman et al., 2018).

### **1.4 The Indus River**

The Indus River originates in the northern slope of the Mount Kailash, close to the Brahmaputra River origin (Figure 1). It initially flows westwards and after partially circumventing the northern flanks of the Nanga Parbat-Haramosh Massif continues flowing to the southwest before discharging into the Arabian Sea (Figure 1, Inam et al., 2007). It is one of the World's largest

ivers and its sediment is mainly eroded from the western Tibetan plateau and Karakorum (Inam et al., 2007). Sediment discharge from the Indus River is smaller than from the Ganges and Brahmaputra rivers (Table 3). It has been estimated that before human intervention in the years 1950-1960, the Indus annually carried 300 to  $675 \cdot 10^9$  kg of sediment of which about  $250 \cdot 10^9$  kg reached the Indus Delta (Milliman et al., 1984). However, the installment of dams along the river reduced the annual sediment discharge by more than 80% (Milliman and Meade, 1983; Giosan et al., 2006).

## 2 Challenges in data comparability and necessary assumptions

### 2.1 Scarcity in sediment measurements from the Indian subcontinent

Measurements of river sediment in the investigated rivers are scarce. We collected data from a variety of studies. However, most of those studies are based on data from sampling stations at the Hardinge Bridge (Ganges River, Table S1) and in Bahadurabad (Brahmaputra River, Table S2). Both of these stations are located after the rivers enter Bangladesh. Generally, sediment data are from river locations close to the delta region and no data from the upper rivers are available (Figure S1). Accordingly, the sediment discharge estimated for these stations yields an average mass loss for the catchments above those locations but no spatial resolution.

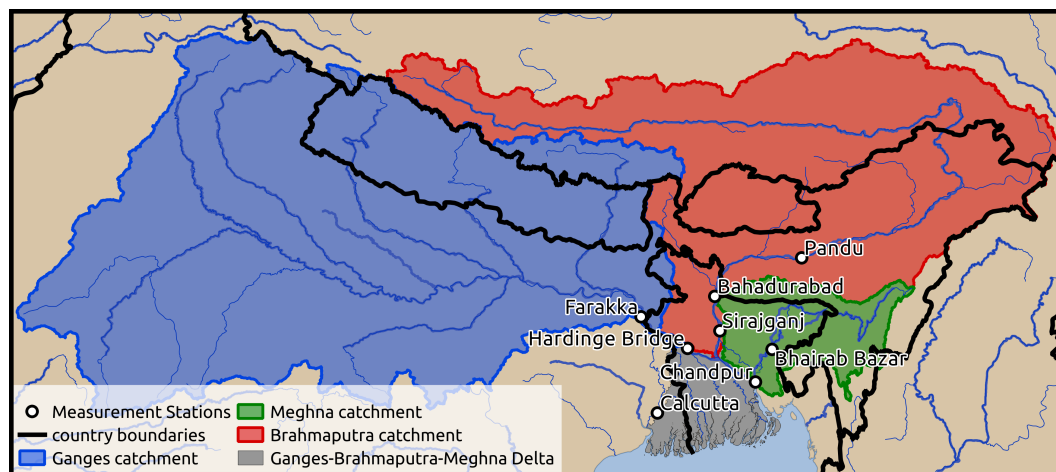


**Figure S1.** Map of Ganges-Brahmaputra-Meghna river system with locations of sediment study locations as stated in Table S1 and Table S2. River locations are from GRDC (2020) and river catchments are from Lehner and Grill (2013).

The river catchments are defined such that they exclude the river delta where a lot of sediment is deposited. This allows a good estimate of net sediment mass loss from the full river system as well as the individual catchments. When studying the mountain regions and floodplains individually, we are dependent on studies of the sediment origin (Faisal and Hayakawa, 2022; Garzanti et al., 2011; Galy et al., 2007; Wasson, 2003). However, those studies find the region where sediment initially originates from and do not provide information on potential deposition and re-distribution of sediment in the floodplains.

Thus, the estimated origin fraction of net sediment mass loss does not necessarily translate to that amount of local mass loss. It is possible that sediment from the mountains is deposited in the floodplains resulting in underestimation of mass loss in the mountains and overestimation of mass loss in the floodplains. The other way around, it is possible that large amounts of previously deposited mountain sediment is transported from the floodplains, resulting in overestimation of mountain sediment mass loss and an underestimation of floodplain sediment mass. Over long time periods, what we derive is likely a minimum estimate of sediment mass loss in the mountains and a maximum estimate of mass loss in the floodplains.

## 2.2 Potential impact of GRACE data filtering and leakage

To suppress GRACE data errors arising from instrument noise, modeling deficiencies and directional model sensitivity, the COST-G data we use are filtered spatially (Mu et al., 2017; Tripathi et al., 2022). This limits the resolution and causes data leakage between the individual grids (Figure S2). Thus, measured EWH loss from one catchment could falsely be attributed to the neighboring one. For the total study area of the combined Ganges, Brahmaputra, Meghna and Indus catchments, this impact is likely negligible. However, considering the main location of EWH loss in north-west India being located at the intersection between the Ganges and Indus catchments, this could yield an error in the attribution of this mass loss between the two catchments.

Additionally, the data leakage softens the impact of small scale local mass loss in individual grids which makes it impossible to observe and validate the potential sediment mass loss in the Indus-Tsangpo suture within the GRACE EWH data. For proper data comparison between sediment mass loss and GRACE EWH, the GRACE filter would need to be applied to the sediment data. However, this would require gridded sediment loss data which are not available.

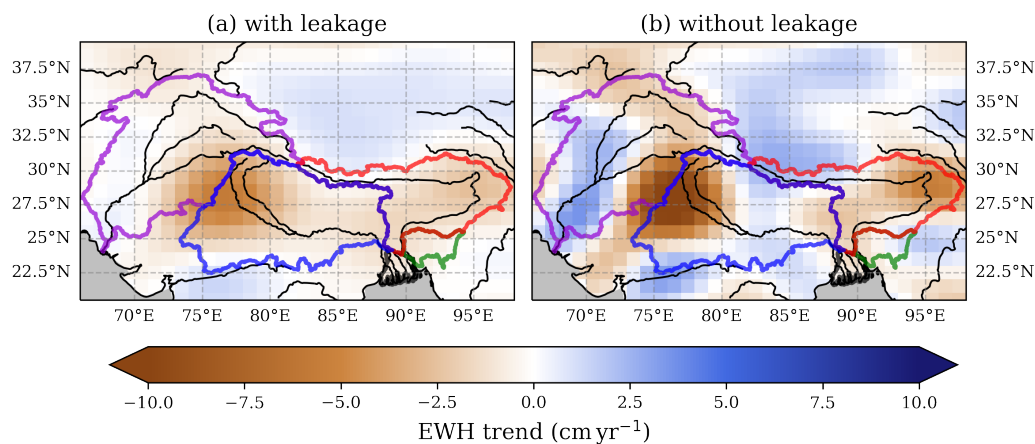


**Figure S2.** Map of the local equivalent water height (EWH) trends within the study are. (a) Including the leakage caused by filtering and (b) without the impact of leakage due to filtering. Data are from the COST-G Level 3 data product (Boergens et al., 2020).

### 3 Discussion of data seasonality

The seasonality of both EWH and river sediment depends on the South Asian monsoon. As such, both parameters follow the seasonality of regional precipitation with the sediment discharge peaking approximately one month after the precipitation maximum and the EWH peaking one month after that (Figure S3). Since the monsoon moves from south-east over the Indian subcontinent, precipitation in the Brahmaputra catchment starts to increase earlier in the year and more gradually, while precipitation in the Ganges catchment starts later and increases more rapidly.

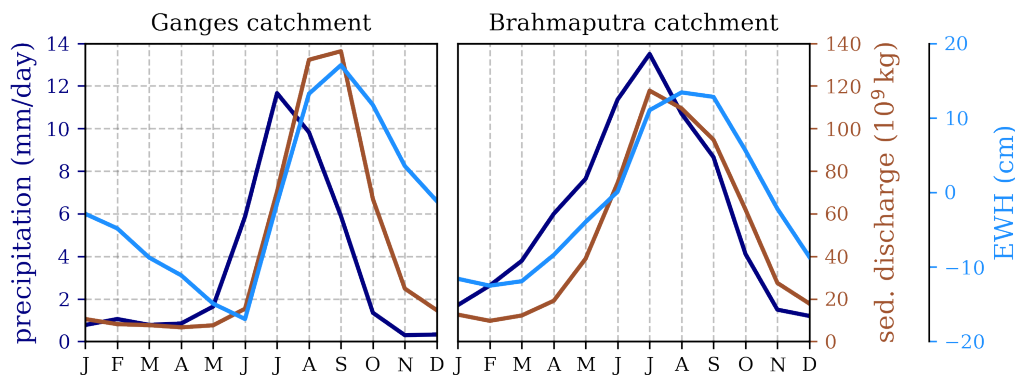


**Figure S3.** Average seasonality of the precipitation (dark blue), the equivalent water height (EWH, light blue), and the sediment discharge (brown) within the Ganges catchment (left) and Brahmaputra catchment (right). Precipitation data are averaged from the ERA5 reanalysis product for 2000-2022 (C3S, 2017). Seasonal EWH data are averaged for the COST-G data product for 2002-2021 Boergens et al. (2020). Seasonality of sediment discharge is based on river water discharge according to data in Islam (2016).

This difference in precipitation patterns is also visible in the sediment discharge and EWH data. For the Brahmaputra River, sediment discharge and EWH in the river catchment yield minima in February and show a gradual increase until the monsoon peak in July (Figure S3). After that, sediment discharge decreases with the precipitation decrease, while EWH stays high until October, when precipitation rates drop below  $5 \text{ mm day}^{-1}$ . For the Ganges River, sediment discharge increases from June to August and decrease from September to November. The EWH in the Ganges catchment rapidly increases between June and August and shows a steady decline from September to June, while the precipitation rate is below  $6 \text{ mm day}^{-1}$  (Figure S3).

### 4 Interpretation of Indus data gap

In the Indus EWH time series, on first glance there appears to be an offset between data from the initial GRACE mission (before 07-2017) and the follow on mission GRACE-FO (after 05-2018, Figure S10). It appears that there is a weaker decline in the data than the linear optimization yields due to a jump to lower EWH during the data gap. However, both the GRACE and GRACE-FO data are calibrated to the same reference fields and should not contain an offset. We decided to look into the Indus catchment in more detail to investigate whether the generated trend is physically reasonable.

Investigation of individual catchment parts yield fairly constant EWH levels in the south-western and northern parts of the Indus catchment. In the northern mountains, there is a strong seasonality with only small inter-annual fluctuation. In the south-western catchment, the seasonality is much weaker, highlighting inter-annual events like the extreme flood in 2010. Neither of these regions show a significant trend or offset between data before and after the data gap (Figure S4). Thus, as shown in the EWH trend map (Figure 2), the main EWH decrease is located in the south-western part of the Indus catchment, where EWH steadily decreases. This decrease speeds up in 2016 and based on this data, a further EWH decrease during the measurement gap in 07-2017 to 05-2018 seems reasonable. The GRACE-FO data yields a fairly stagnant EWH levels until the end of 2020. We conclude that the observed trend, while in reality not being linear, seems physically reasonable and continue to use it in our study.

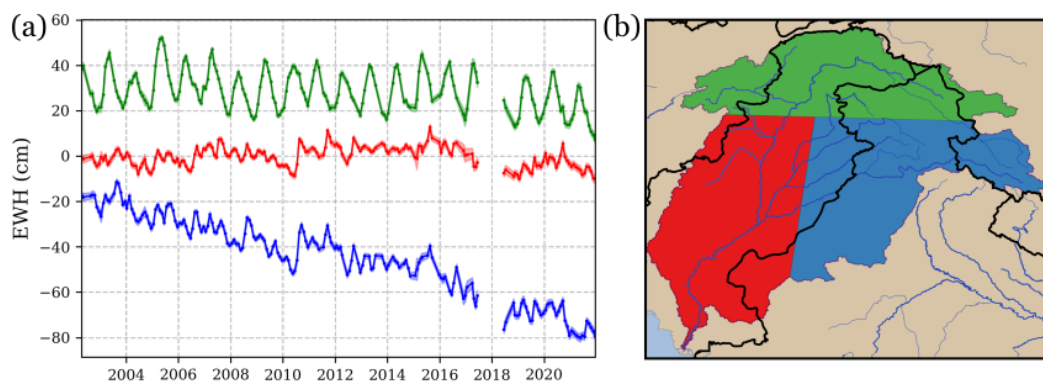


**Figure S4.** Equivalent water height (EWH) trends for different segments of the Indus catchment. (a) EWH trends for the northern (green), south-western (red), and south-eastern (blue) part of the Indus catchment. Data for the northern and south-eastern parts are adapted by an offset of 30 cm and  $-40$  cm, respectively. (b) Map of the segment separation. A similar visualization for the Ganges catchment can be found in Figure S12.

## 5 Additional figures and tables

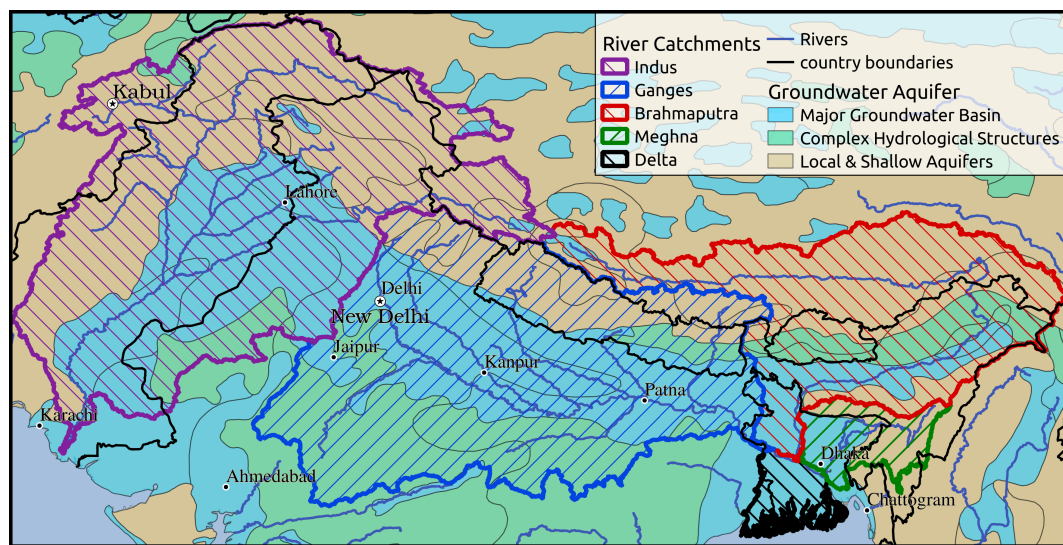


**Figure S5.** Map of study area with location and type of groundwater aquifers from EHYMAP RGWB (2010), river locations from GRDC (2020) and river catchments from Lehner and Grill (2013).

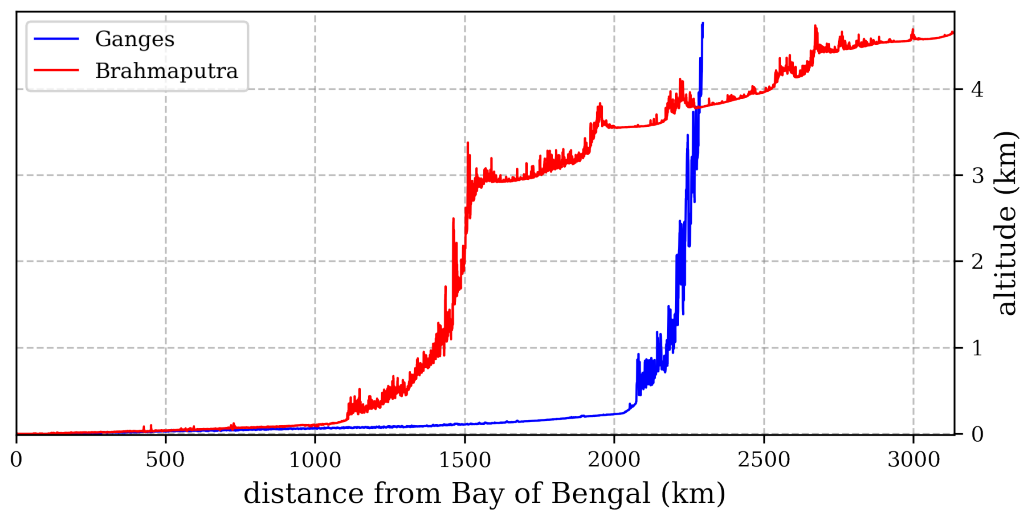


**Figure S6.** Profiles for the main branches of the Ganges and Brahmaputra rivers. Elevation is derived from data of Jarvis et al. (2008). River paths are as defined in GRDC (2020).

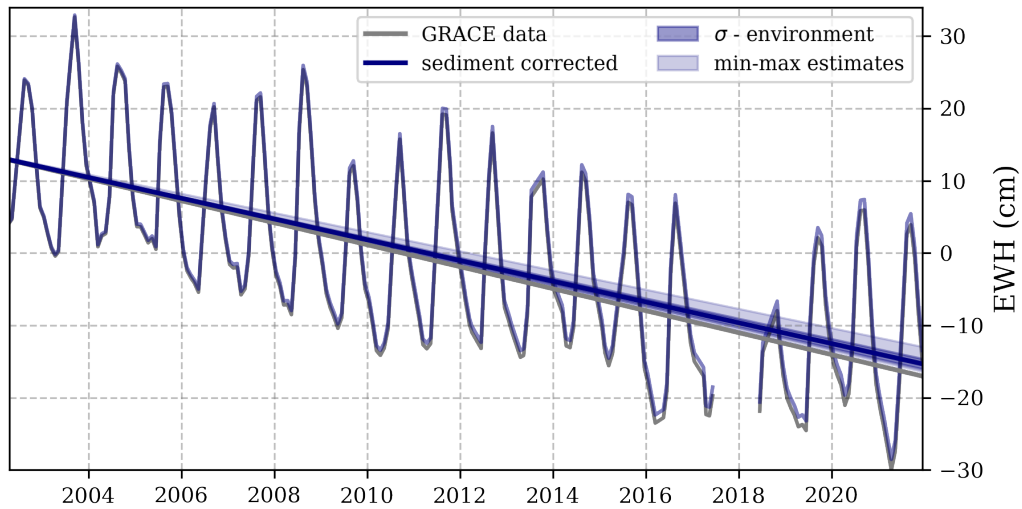


**Figure S7.** Time series of EWH derived from GRACE data and EWH corrected for sediment mass loss. Data show average over the whole Ganges-Brahmaputra-Meghna catchments.

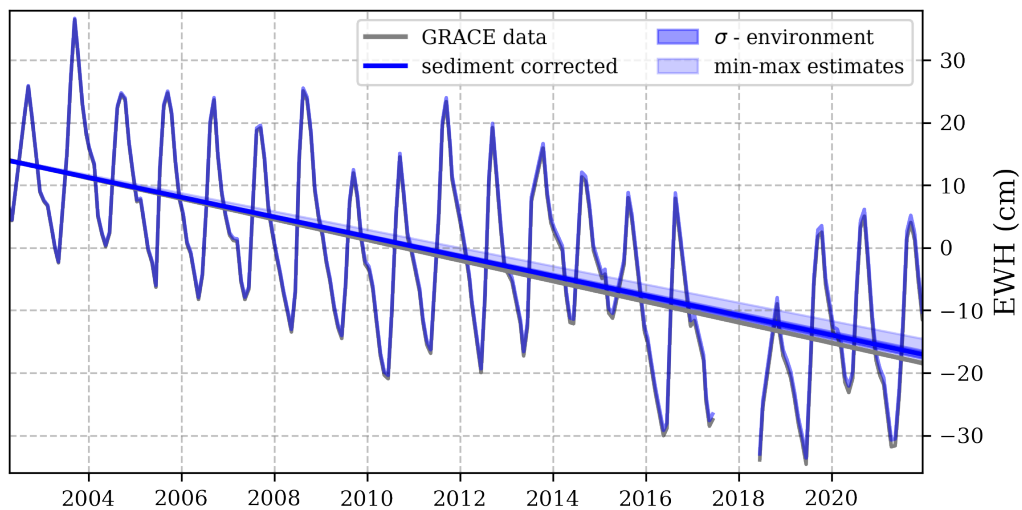


**Figure S8.** Time series of EWH derived from GRACE data and EWH corrected for sediment mass loss. Data show average over the whole Ganges catchment.

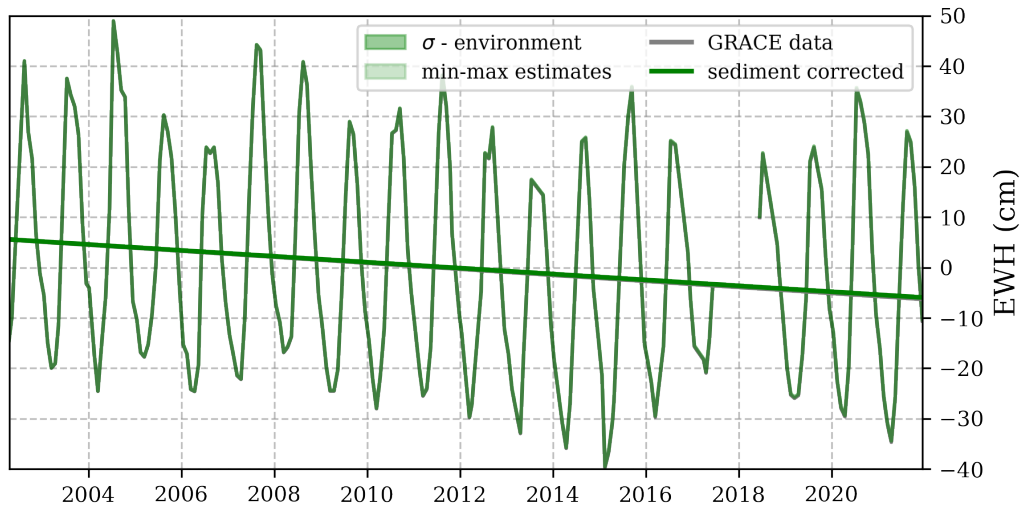


**Figure S9.** Time series of EWH derived from GRACE data and EWH corrected for sediment mass loss. Data show average over the whole Meghna catchment.

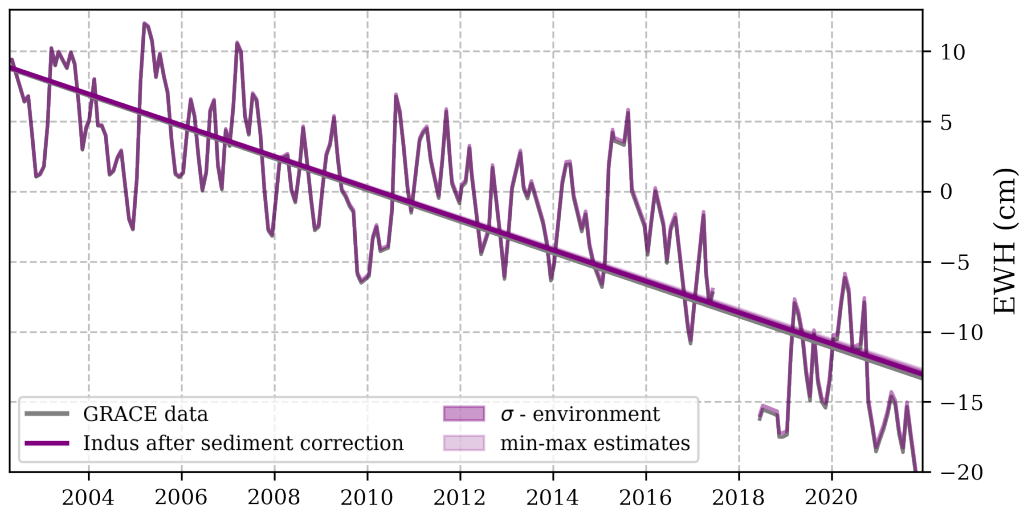


**Figure S10.** Time series of EWH derived from GRACE data and EWH corrected for sediment mass loss. Data show average over the whole Indus catchment.

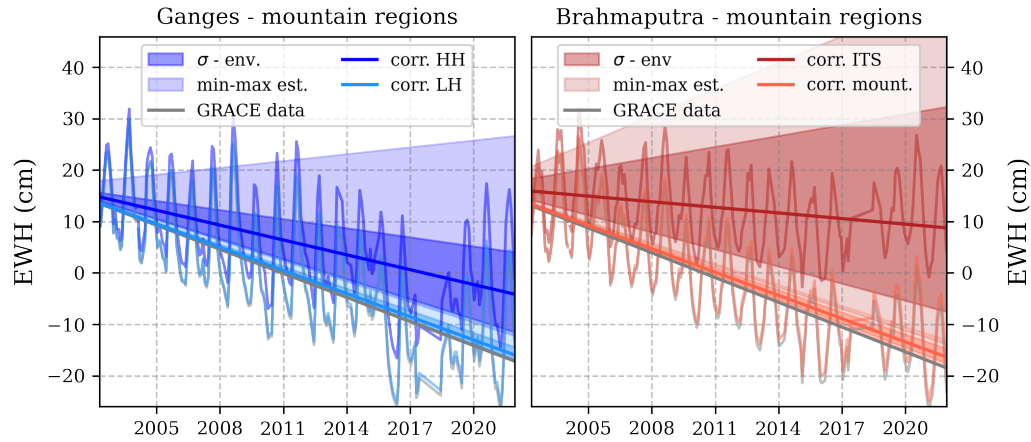


**Figure S11.** Time series of EWH derived from GRACE data and EWH after the correction for sediment mass loss. EWH data is derived as the average over the mountain fraction within the Ganges catchment (left) and the Brahmaputra catchment (right). For the Ganges catchment, the sediment correction is derived locally for the High Himalayas (HL,  $\approx 57,976 \text{ km}^2$ ) and the Lesser Himalayas (LH,  $\approx 93,416 \text{ km}^2$ ). These regions were defined analogous to Faisal and Hayakawa (2022). For the Brahmaputra catchment, the sediment correction is derived locally for the Indus-Tsangpo suture (ITS,  $\approx 21,600 \text{ km}^2$ ) and the remaining mountain fraction (mount.,  $\approx 339,900 \text{ km}^2$ ). The  $\sigma$  environment and min-max estimates refer to the sediment discharge as stated in Table 3.

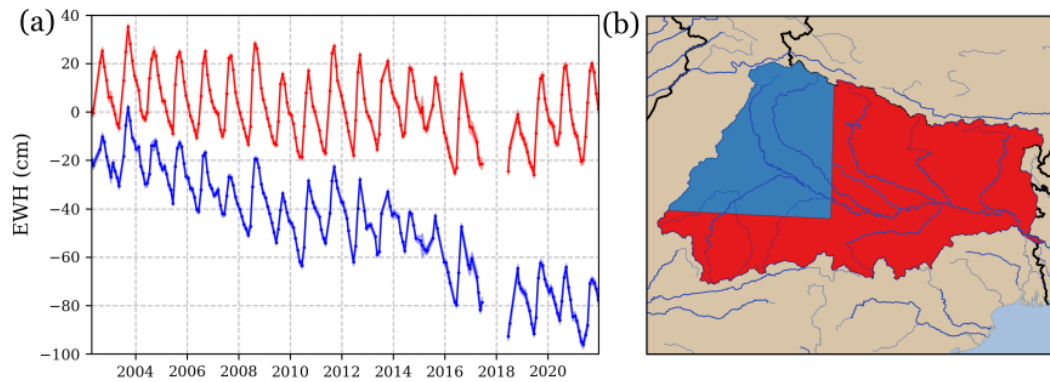


**Figure S12.** Equivalent water height (EWH) trends for different segments of the Ganges catchment. a) EWH trends for the north-western (blue), and south-eastern (red) part of the Ganges catchment. Data are adapted by an offset of  $-42 \text{ cm}$  and  $2 \text{ cm}$ , respectively. b) Map of the segment separation.

**Table S1.** Estimates of sediment load in the Ganges River from different literature studies.

susp. sediment ( $10^9$ kg yr <sup>-1</sup> )	time period	location	source
210	unknown	Hardinge Bridge	MPO (1987) in Rahman et al. (2018)
340	unknown	Hardinge Bridge	FEC (1989) in Rahman et al. (2018)
430-729	unknown	unknown	Thakkar (2006)
550	unknown	unknown	CEGIS (2010) in Rahman et al. (2018)
1600	1874-1879	Hardinge Bridge	Holeman (1968)
478.9 (257-736)	1958-1962	Hardinge Bridge	Coleman (1969)
375	1960	unknown	NEDECO (1967) in Islam et al. (1999)
680 <sup>(a)</sup>	1966-1967	Hardinge Bridge	Milliman and Meade (1983)
520	1966-1969	Hardinge Bridge	BWDB (1972) in Islam et al. (1999)
548	1966-1970	Hardinge Bridge	WARPO (1996) in Rahman et al. (2018)
548	1966-1970	Hardinge Bridge	DH and DHI (1991) in Lupker et al. (2011)
200	1965-1988	Hardinge Bridge	CBJE (1991) in Rahman et al. (2018)
487	1976-1989	Hardinge Bridge	Tarekul Islam and Jaman (2006)
328	1981	Calcutta	Abbas and Subramanian (1984)
729	1981	Farakka	Abbas and Subramanian (1984)
403	1983-1984	Farakka	Singh (1988)
480 (350-600)	1980-1986	Hardinge Bridge	Hossain (1992) in Rahman et al. (2018)
502	1989-1991	Bengal Delta	Barua et al. (1994)
316 (155-863)	1979–1995	Hardinge Bridge	Islam et al. (1999)
216-1038	1981-2001	Hardinge Bridge	Akter et al. (2021)
150-590	1960-2008	Hardinge Bridge	Rahman et al. (2018)
262	2006	Hardinge Bridge	Rice (2007)
390 (360-420)	2004-2010	Hardinge Bridge	Lupker et al. (2011)

This set of estimates was build upon collections in Islam et al. (1999), Rahman et al. (2018) and Faisal and Hayakawa (2022). <sup>(a)</sup> Value for Ganges River taken from Islam et al. (1999). Original study states  $1670 \cdot 10^9$  kg yr<sup>-1</sup> after Ganges-Brahmaputra confluence.

**Table S2.** Estimates of sediment load in the Brahmaputra River from different literature studies.

Suspended sediment ( $10^9 \text{ kg yr}^{-1}$ )	time period	location	source
390	unknown	unknown	MPO (1987) in Rahman et al. (2018)
800	unknown	unknown	Holeman (1968)
710	unknown	unknown	Subramanian (1987) in Islam et al. (1999)
430	unknown	Bahadurabad	FEC (1989) in FEC (1989)
590	unknown	unknown	CEGIS (2010) in Rahman et al. (2018)
402	1955-1979	Pandu	Goswami (1985)
607.7 (531-697)	1958-1962	Bahadurabad	Coleman (1969)
750	1960	unknown	NEDECO (1967) in Islam et al. (1999)
1157 <sup>(a)</sup>	1966-1967	Bahadurabad	Milliman and Meade (1983)
541	1966-1969	Bahadurabad	BWDB (1972) in Islam et al. (1999)
80-228	1981-2001	Bahadurabas	Akter et al. (2021)
500	1965-1988	Bahadurabad	CBJE (1991) in Rahman et al. (2018)
650 (400-850)	1980-1986	Bahadurabad	Hossain (1992) in Rahman et al. (2018)
1028	1989-1991	Bahadurabad	Barua et al. (1994)
721 (455-992)	1989–1994	Bahadurabad	Islam et al. (1999)
541	1993	Bahadurabad	Kabir and Ahmed (1996) in Rahman et al. (2018)
135-615	1960-2008	Bahadurabad	Rahman et al. (2018)
387	2006	Sirajganj	Rice (2007)

The set of estimates was build upon collections in Islam et al. (1999), Rahman et al. (2018) and Faisal and Hayakawa (2022)). <sup>(a)</sup> Value for Brahmaputra River taken from Islam et al. (1999). Original study states  $1670 \cdot 10^9 \text{ kg yr}^{-1}$  after Ganges-Brahmaputra confluence.

## References

- Abbas, N. and Subramanian, V.: Erosion and sediment transport in the Ganges river basin (India), *Journal of Hydrology*, 69, 173–182, [https://doi.org/10.1016/0022-1694\(84\)90162-8](https://doi.org/10.1016/0022-1694(84)90162-8), 1984.
- Akhtar, M. K., Corzo, G. A., van Andel, S. J., and Jonoski, A.: River flow forecasting with artificial neural networks using satellite observed precipitation pre-processed with flow length and travel time information: case study of the Ganges river basin, *Hydrology and Earth System Sciences*, 13, 1607–1618, <https://doi.org/10.5194/hess-13-1607-2009>, 2009.
- Akter, J., Roelvink, D., and van der Wegen, M.: Process-based modeling deriving a long-term sediment budget for the Ganges-Brahmaputra-Meghna Delta, Bangladesh, *Estuarine, Coastal and Shelf Science*, 260, 107 509, <https://doi.org/10.1016/j.ecss.2021.107509>, 2021.
- Barua, D. K., Kuehl, S. A., Miller, R. L., and Moore, W. S.: Suspended sediment distribution and residual transport in the coastal ocean off the Ganges-Brahmaputra river mouth, *Marine Geology*, 120, 41–61, [https://doi.org/10.1016/0025-3227\(94\)90076-0](https://doi.org/10.1016/0025-3227(94)90076-0), tidal and Shallow-Sea Sediments-Modern Environments, 1994.
- Boergens, E., Dobslaw, H., and Dill, R.: COST-G GravIS RL01 Continental Water Storage Anomalies. V. 0004., GFZ Data Services., [https://doi.org/10.5880/COST-G.GRAVIS\\_01\\_L3\\_TWS](https://doi.org/10.5880/COST-G.GRAVIS_01_L3_TWS), accessed 20.12.2022, 2020.
- BWDB: Sediment investigations in Main Rivers of Bangladesh, 1968 & 1969, BWDB Water Supply Paper No. 359., (Bangladesh Water Development Board), 1972.
- C3S: Copernicus Climate Change Service (C3S): ERA5: Fifth generation of ECMWF atmospheric reanalyses of the global climate., Copernicus Climate Change Service Climate Data Store (CDS), <https://cds.climate.copernicus.eu/cdsapp#!/home>, accessed 14.06.2022, 2017.
- CBJE: Study Report on Flood Control and River Training Project on the Brahmaputra River in Bangladesh, Vol. 1 and Vol. 2, Government of Peoples Republic of China and Government of Bangladesh, Beijing and Dhaka, (China-Bangladesh Joint Expert Team), 1991.
- CEGIS: Impact of Climate Change on Morphological Processes in Different River of Bangladesh, Prepared for Asian Development Bank, Dhaka, Bangladesh, (Center for Environmental and Geographic Information Services), 2010.
- Coleman, J. M.: Brahmaputra river: Channel processes and sedimentation, *Sedimentary Geology*, 3, 129–239, [https://doi.org/10.1016/0037-0738\(69\)90010-4](https://doi.org/10.1016/0037-0738(69)90010-4), brahmaputra river: Channel processes and sedimentation, 1969.
- DH and DHI: River Survey Project, Flood Action Plan 24, Water Resour. Plann. Org., Dhaka, (Delft Hydraulics and Danish Hydraulics Institute), 1991.
- EHYMAP RGWB: River and Groundwater Basins of the World (WHYMAP RGWB) v1.0, The World-wide Hydrogeological Mapping and Assessment Programme (WHYMAP): River and Groundwater Basins of the World (RGWB), accessed via <https://produktcenter.bgr.de/terraCatalog/OpenSearch.do?search=54e5d435-ac3f-4d2e-9e42-bd77728c1e05&type=/Query/OpenSearch.do> (17.11.2022), 2010.
- Faisal, B. M. R. and Hayakawa, Y. S.: Geomorphological processes and their connectivity in hillslope, fluvial, and coastal areas in Bangladesh: A review, *Progress in Earth and Planetary Science*, 9, <https://doi.org/10.1186/s40645-022-00500-8>, 2022.
- FEC: Pre-Feasibility Study for Flood Control in Bangladesh, vol. 2, Present Conditions, Paris, (French Engineering Consortium), 1989.
- Galy, V., France-Lanord, C., Beyssac, O., Faure, P., Kudrass, H., and Palhol, F.: Efficient organic carbon burial in the Bengal fan sustained by the Himalayan erosional system, *Nature*, 450, <https://doi.org/10.1038/nature06273>, 2007.
- Garzanti, E., Andó, S., France-Lanord, C., Censi, P., Vignola, P., Galy, V., and Lupker, M.: Mineralogical and chemical variability of fluvial sediments 2. Suspended-load silt (Ganga–Brahmaputra, Bangladesh), *Earth and Planetary Science Letters*, 302, 107–120, <https://doi.org/10.1016/j.epsl.2010.11.043>, 2011.

- Giosan, L., Constantinescu, S., Clift, P. D., Tabrez, A. R., Danish, M., and Inam, A.: Recent morphodynamics of the Indus delta shore and shelf, *Continental Shelf Research*, 26, 1668–1684, <https://doi.org/10.1016/j.csr.2006.05.009>, 2006.
- Goswami, D. C.: Brahmaputra River, Assam, India: Physiography, Basin Denudation, and Channel Aggradation, *Water Resources Research*, 21, 959–978, <https://doi.org/10.1029/WR021i007p00959>, 1985.
- GRDC: Major River Basins of the World: "Major Rivers", Global Runoff Data Centre. 2nd, rev. ext. ed. Koblenz, Germany: Federal Institute of Hydrology (BfG), accessed via: [https://www.bafg.de/SharedDocs/ExterneLinks/GRDC/mrb\\_shp\\_zip.html;jsessionid=993792470F4B2723B3942ACFA8C09C66.live11313?nn=201762](https://www.bafg.de/SharedDocs/ExterneLinks/GRDC/mrb_shp_zip.html;jsessionid=993792470F4B2723B3942ACFA8C09C66.live11313?nn=201762) (24.10.2022)., 2020.
- Holeman, J. N.: The Sediment Yield of Major Rivers of the World, *Water Resources Research*, 4, 737–747, <https://doi.org/10.1029/WR004i004p00737>, 1968.
- Hossain, M.: Total sediment load in the lower Ganges and Jamuna, *J. Inst. Engrs. Bangladesh*, 20, 1 – 8, <https://www.scopus.com/inward/record.uri?eid=2-s2.0-0342490796&partnerID=40&md5=822d0234ae1a00fb7f29cd21c2f7e563>, 1992.
- Inam, A., Clift, P. D., Giosan, L., Tabrez, A. R., Tahir, M., Rabbani, M. M., and Danish, M.: The Geographic, Geological and Oceanographic Setting of the Indus River, chap. 16, pp. 333–346, John Wiley & Sons, Ltd, <https://doi.org/10.1002/9780470723722.ch16>, 2007.
- Islam, M. R., Begum, S. F., Yamaguchi, Y., and Ogawa, K.: The Ganges and Brahmaputra rivers in Bangladesh: basin denudation and sedimentation, *Hydrological Processes*, 13, 2907–2923, [https://doi.org/10.1002/\(SICI\)1099-1085\(19991215\)13:17<2907::AID-HYP906>3.0.CO;2-E](https://doi.org/10.1002/(SICI)1099-1085(19991215)13:17<2907::AID-HYP906>3.0.CO;2-E), 1999.
- Islam, S.: Deltaic floodplains development and wetland ecosystems management in the Ganges–Brahmaputra–Meghna Rivers Delta in Bangladesh, *Sustainable Water Resources Management*, 2, <https://doi.org/10.1007/s40899-016-0047-6>, 2016.
- Jarvis, A., Reuter, H., Nelson, A., and Guevara, E.: Hole-filled seamless SRTM data V4, International Centre for Tropical Agriculture (CIAT), accessed from <https://srtm.csi.cgiar.org> (24.10.2022)., 2008.
- Kabir, M. and Ahmed, N.: Bed shear stress for sediment transportation in the River Jamuna, *Journal of Civil Engineering, The Institution of Engineers, Bangladesh*, 24 CE, 55 – 68, <https://www.scopus.com/inward/record.uri?eid=2-s2.0-84892444734&partnerID=40&md5=1d4dbda20f2a153bd21c6a1f58db1348>, 1996.
- Lehner, B. and Grill, G.: Global river hydrography and network routing: baseline data and new approaches to study the world's large river systems., <https://doi.org/10.1002/hyp.9740>, accessed via <https://www.hydrosheds.org/products/hydrobasins> (20.10.2022), 2013.
- Lupker, M., France-Lanord, C., Lavé, J., Bouchez, J., Galy, V., Métivier, F., Gaillardet, J., Lartiges, B., and Mugnier, J.-L.: A Rouse-based method to integrate the chemical composition of river sediments: Application to the Ganga basin, *Journal of Geophysical Research: Earth Surface*, 116, <https://doi.org/10.1029/2010JF001947>, 2011.
- Milliman, J., Quraishie, G., and Beg, M.: Sediment discharge from the Indus River to the ocean: past, present and future, *Marine geology and oceanography of Arabian Sea and coastal Pakistan*, pp. 65–70, 1984.
- Milliman, J. D. and Meade, R. H.: World-Wide Delivery of River Sediment to the Oceans, *The Journal of Geology*, 91, 1–21, <http://www.jstor.org/stable/30060512>, 1983.
- MPO: Floods and storms, Tech. Rep. 11, (Master Plan Organization), 1987.
- Mu, D., Yan, H., Feng, W., and Peng, P.: GRACE leakage error correction with regularization technique: case studies in Greenland and Antarctica, *Geophysical Journal International*, 208, 1775–1786, <https://doi.org/10.1093/gji/ggw494>, 2017.
- NEDECO: East Pakistan Inland Water Transport Authority: Surveys of Inland Waterways and Ports 1963–1967, *Hydrographic Manual*, (Netherlands Engineering Consultants), 1967.

- Paszkowski, A., Goodbred, S., Borgomeo, E., Khan, M. S. A., and Hall, J. W.: Geomorphic change in the Ganges–Brahmaputra–Meghna delta, *Nature Reviews Earth & Environment*, 2, <https://doi.org/10.1038/s43017-021-00213-4>, 2021.
- Rahman, M., Dustegir, M., Karim, R., Haque, A., Nicholls, R. J., Darby, S. E., Nakagawa, H., Hossain, M., Dunn, F. E., and Akter, M.: Recent sediment flux to the Ganges-Brahmaputra-Meghna delta system, *Science of The Total Environment*, 643, 1054–1064, <https://doi.org/10.1016/j.scitotenv.2018.06.147>, 2018.
- Rice, S. K.: Suspended Sediment Transport in the Ganges-Brahmaputra River System, Bangladesh, Master's thesis, Texas A & M University, 2007.
- Singh, S. K.: Nature of chemical and sediment load in the Ganges River between Sone and Kosi, Ph.D. thesis, Jawaharlal Nehru University, New Delhi, India, <http://hdl.handle.net/10603/16314>, 1988.
- Subramanian, V.: Environmental geochemistry of Indian river basins - a review., *Journal of the Geological Society of India*, 29, 205 – 220, <https://www.scopus.com/inward/record.uri?eid=2-s2.0-0023159471&partnerID=40&md5=9ef05ffa095d623bcc21a195a1f8ea24>, 1987.
- Tarekul Islam, G. M. and Jaman, S. T.: Modelling sediment loads in the Lower Ganges, Bangladesh, *Proceedings of the Institution of Civil Engineers - Water Management*, 159, 87–94, <https://doi.org/10.1680/wama.2006.159.2.87>, 2006.
- Thakkar, H.: What, who, how and when of experiencing floods as a disaster, *Issues*, 20, 1 – 37, <https://www.scopus.com/inward/record.uri?eid=2-s2.0-84920029256&partnerID=40&md5=5ad08ce56e55b9346fd5fd67df83df0d>, 2006.
- Tripathi, V., Groh, A., Horwath, M., and Ramsankaran, R.: Scaling methods of leakage correction in GRACE mass change estimates revisited for the complex hydro-climatic setting of the Indus Basin, *Hydrology and Earth System Sciences*, 26, 4515–4535, <https://doi.org/10.5194/hess-26-4515-2022>, 2022.
- WARPO: Sediment Rating Curves and Balances, Special Report No. 18 River Survey Project, Dhaka, Bangladesh, (Water Resources Planning Organization), 1996.
- Wasson, R. J.: A sediment budget for the Ganga–Brahmaputra catchment, *Current Science*, 84, 1041–1047, <http://www.jstor.org/stable/24107666>, 2003.